

Project

Oil Leakage Paths within Compressors of Jet Engines and Oil Concentration in Aircraft Cabin Air

Author: Dennis Tietke

Supervisor: Prof. Dr.-Ing. Dieter Scholz, MSME
Submitted: 25.03.2020

*Faculty of Engineering and Computer Science
Department of Automotive and Aeronautical Engineering*

DOI:

<https://doi.org/10.15488/19107>

URN:

<https://nbn-resolving.org/urn:nbn:de:gbv:18302-aero2020-03-25.017>

Associated URLs:

<https://nbn-resolving.org/html/urn:nbn:de:gbv:18302-aero2020-03-25.017>

© This work is protected by copyright

The work is licensed under a Creative Commons Attribution-NonCommercial-ShareAlike 4.0 International License: CC BY-NC-SA

<https://creativecommons.org/licenses/by-nc-sa/4.0>



Any further request may be directed to:

Prof. Dr.-Ing. Dieter Scholz, MSME

E-Mail see: <http://www.ProfScholz.de>

This work is part of:

Digital Library - Projects & Theses - Prof. Dr. Scholz

<http://library.ProfScholz.de>

Published by

Aircraft Design and Systems Group (AERO)

Department of Automotive and Aeronautical Engineering

Hamburg University of Applied Science

This report is deposited and archived:

- Deutsche Nationalbibliothek (<https://www.dnb.de>)
 - Repository of Leibniz University Hannover (<https://www.repo.uni-hannover.de>)
 - Internet Archive (<https://archive.org>)
- Item: <https://archive.org/details/TextTietke.pdf>

This report has associated published data in Harvard Dataverse:

<https://doi.org/10.7910/DVN/0U73NV>

Abstract

Purpose – Investigation of oil leakage paths from the engine seals into the gas path of jet engine compressors and the estimation of oil concentration in aircraft cabin air based on fundamental aircraft and engine parameters.

Approach – Real jet engine illustrations were collected and used for a detailed investigation of possible paths of oil-contaminated air into the main gas stream of the jet engine compressor before the extraction of bleed air. Furthermore, an equation was analyzed to calculate the oil concentration in the cabin air. Required aircraft and engine parameters were collected for five engines: CF34, V2500, CFM56, PW4000, and GE90 on typical aircraft.

Findings – On the basis of the illustrations various oil leakage paths were identified. Regarding the oil concentration, it could be shown that larger engines tend to have lower oil concentration in the cabin air. If the position of the bleed port for bleed air extraction is located further downstream with respect to the engine seals, oil concentration is higher.

Research Limitations – All investigations are based on common sense. The oil concentration in the cabin was calculated based on the assumption that 1 % of oil consumption goes into the cabin.

Practical Implications – The influence of fundamental aircraft and engine parameters on oil concentration is better understood. These parameters are number of engines, engine air intake diameter, by-pass ratio, total number of bearings (seals) and their number upstream of the bleed port, oil consumption, cruise Mach number, and cruise altitude.

Social Implications – People concerned about aircraft cabin air contamination can better argue their case with the information in this project.

Value – It is an important step in the argument to show how the oil can find its way into the compressed air path. Before, it was just assumed that leaking oil from the engine seals will "somehow" make its way. The usefulness of the equation for oil concentration in the cabin air is shown now with an increased number of five engines instead of just one engine as before. This gives increased credibility to the equation.

Keywords:

aviation, aircraft, cabin, air, contamination, event, CACE, smoke, fume, fume event, engine, jet engine, oil, consumption, leakage, compressor, bearing, bearing chamber, seal, path, bleed air

Oil Leakage Paths within Compressors of Jet Engines and Oil Concentration in Aircraft Cabin Air

Task for a *Project*

Background

Cabin Air Contamination (details here: <http://CabinAir.ProfScholz.de>) is caused by leakage through the seals of jet engines. Jet engines have heavy shafts supported by bearings. They are lubricated and sealed. These seals leak small amounts of oil by design. The leakage related concentration of hydrocarbons in the cabin depends not only on the amount of oil leaving the seals, but also on a set of engine and aircraft parameters, because not all the oil can reach the cabin. The parameters are combined in one simple equation. We look at several dominant jet aircraft and their engines in order to calculate the cabin air contamination potential. A comparison may reveal aircraft-engine-combinations more prone to cabin air contamination than others based already on external design parameters. Furthermore, we look at the jet engine design in more detail to understand, how the oil finds its way from leaking seals into the main gas path of the jet engine compressor and finally via the bleed port into the cabin.

Task

Task of this project is to study and analyze details of engine oil leakages in jet engines and their consequences to oil concentration in aircraft cabin air. The subtasks are:

- Collect design drawings of jet engines.
- Study one or more possible paths for the oil to reach the cabin from leaking seals.
- Collect data on oil consumption of jet engines.
- Collect aircraft and engine parameters as required to calculate the concentration of the oil in aircraft cabin air.
- Calculate and analyze concentration of the oil in the aircraft cabin air of various aircraft and engine combinations and draw general conclusions.

The report has to be written in English based on German or international standards on report writing.

Table of Contents

	page
List of Figures	6
List of Tables.....	6
List of Symbols	7
List of Abbreviations.....	7
1 Introduction	8
1.1 Motivation	8
1.2 Objectives	8
1.3 Structure	8
2 Fundamentals.....	10
3 Possible Path of Lubricating Oil in an Aircraft Engine.....	13
4 Volume and Mass Flow Rates in the Bearing Chamber and Breather	23
5 Evaluation of Design Parameters.....	27
6 Summary and Conclusions	32
List of References	33

List of Figures

Figure 2.1	Bleed valve position CFM56 engine (Adapted from CFMI 2000).....	11
Figure 2.2	Typical air distribution (Lufthansa 2015).....	11
Figure 2.3	Pratt & Whitney PW4000 engine (Pratt & Whitney 2014)	12
Figure 3.1	Lubrication system (Linke-Diesinger 2014).....	13
Figure 3.2	Bearing sump in lubrication system (Otis 1997)	14
Figure 3.3	Typical bearing sump (Kroes 1994)	14
Figure 3.4	labyrinth seal with leakage flow (Flitney 2014)	15
Figure 3.5	Carbon seal (Chupp 2006)	16
Figure 3.6	JT8D air path (adapted from Treager 1995)	17
Figure 3.7	JT8D bearing sump (adapted from Treager 1995).....	18
Figure 3.8	Detailed view of JT8D bearing (adapted from Treager 1995).....	19
Figure 3.9	CF6 sump "A" (Otis 1997)	19
Figure 3.10	JT9D forward bearing (adapted from Kroes 1994).....	20
Figure 3.11	JT9D main gas stream(adapted from Kroes 1994)	21
Figure 3.12	Bearing two of the T58 jet engine (adapted from Treager 1995)	22
Figure 4.1	Bearing chamber two-phase flow (Kurz 2012).....	23
Figure 4.2	De-aerator, de-oiler (Cordes 2017).....	24
Figure 4.3	Air/Oil Separator CFM56-5A (adapted from CFMI 2000)	24
Figure 4.4	Volume/mass flow bearing chamber	25
Figure 5.1	Bearing sump CFM56 (LTT 1999).....	29
Figure 5.2	Front bearing sump CFM56 (Linke-Diesinger 2014).....	30
Figure 5.3	Detailed front sump CFM56 (adapted from Scripd 2020).....	30

List of Tables

Table 4.1	Conclusion of values from Figure 4.4.....	26
Table 5.1	Oil consumption for different engine types	27
Table 5.2	Calculation of the Oil Concentration in the Cabin.....	28

List of Symbols

a	Speed of sound
h	Aircraft cruise altitude
m	Mass
\dot{m}	Mass flow rate
n	Quantity
S	Engine intake area
V	Volume
x	Ratio

Greek Symbols

μ	By-Pass Ratio
ρ	Density

List of Subscripts

bear, up	Bearing Upstream
cab	Cabin
CR	Cruise Altitude
eng	Engine
oil	Oil
oil, cab	Oil in Cabin
seal	(Oil-)Seal

List of Abbreviations

APU	Auxiliary Power Unit
CACE	Cabin Air Contamination Event
CFM	General Electric CF6 and Snecma M56
GE	General Electric
PW	Pratt & Whitney
RR	Rolls-Royce

1 Introduction

1.1 Motivation

Due to the high number of aircraft movements worldwide, so-called Fume Events occur every day. Lubricating oil from the engine bearings enters the main gas flow of the jet engine. Once reaching a point before the bleed air is extracted, the lubricating oil may flow into the aircraft cabin in a gaseous state. The source of the lubricating oil, the bearing chamber, is part of the complex design of an engine. This system is used to enable rotation of the engine shafts and is located at the core of the engine. It is difficult to visualize how the oil mist passes from this central location into the main gas flow. Videos of Fume Events demonstrate smoke-contaminated aircraft cabins and lead to the question of how much lubricating oil gets into the bleed air for the cabin. An invisible contamination of the air is not an indicator that the air is free of lubrication oil. A calculation of the oil concentration in the cabin air as a function of engine and flight parameters gives an impression of the amount of oil in the aircraft cabin. Thus, an assessment of the contamination is even possible without the presence of visible Fumes.

1.2 Objectives

The main objective of this report is to determine the path of the lubricating oil from the bearing chamber of the jet engine to the main gas stream and thus to the bleed air. Furthermore, one specific parameter will be analyzed and discussed that is part of an equation to estimate the oil concentration in the aircraft cabin air. In addition, various oil concentrations are presented and analyzed for different engine types.

1.3 Structure

Chapter 2 explains the phenomenon of contaminated cabin air in aircraft cabins. It briefly explains where the sources of contamination are located and displays the path the air is expected to take from the engines to the cabin.

Chapter 3 is dedicated to an exact description of the bearing sumps of an engine, as well as their construction. The possible path of lubricating oil into the main gas flow of the engine is shown using schematic illustrations of real engines.

- Chapter 4** gives an overview of the volume and mass flows in a breather, based on a literature review. The results are presented graphically.
- Chapter 5** focuses on the analysis of some parameters that are used for an approximate calculation of the oil concentration in the cabin air. Furthermore, some calculations show the result for different jet engine types.

2 Fundamentals

Almost every day a Cabin Air Contamination Event (CACE) happens to an aircraft in the United States. (Murawski 2008) assumes at least 0.86 events per day, although this assumption is very conservative, and the number of unreported events will even be higher. A CACE event describes a Fume or Smell event. In terms of contaminated cabin air, a Fume event is a potentially toxic environment in the cabin where the bleed air is considered the source (Day 2015). A Smell Event is similar to a Fume Event, but the contaminations are not visible to human eyes.

One of the main causes of contaminated bleed air has been identified as bearing sump leakage (Michaelis 2018). Bearing sumps are areas where the engine shafts or the shaft of an Auxiliary Power Unit (APU) are supported by roller bearings. These bearings must be constantly supplied with lubricating oil. The main function of lubricating oil is to reduce friction between the bearing components and to dissipate heat generated by the high rotational speed of the bearings. (Linke-Diesinger 2014) The bearing sumps are sealed by oil seals which ensure that as little oil as possible can leave the bearing sump. The following sentence describes the problem of sealing.

„A zero-leakage seal is an oxymoron” (Chupp 2006)

It is not possible to design seals so that no oil escapes from a bearing sump.

If the lubricating oil has leaked from the sump, there is a possibility that the oil will enter the bleed ports for the cabin air. Bleed ports are connections in the main gas flow of the engine. Since the engine has different conditions in a flight cycle, there are at least two bleed valves within an engine.

Figure 2.1 shows the high-pressure compressor of the CFM56 engine. The bleed air for cruise is extracted after the fifth stator stage. For flight conditions that require less power, the bleed air is taken from the main gas flow after a few compressor stages. On the CFM56 engine this is done after the ninth rotor stage. (Linke-Diesinger 2014)

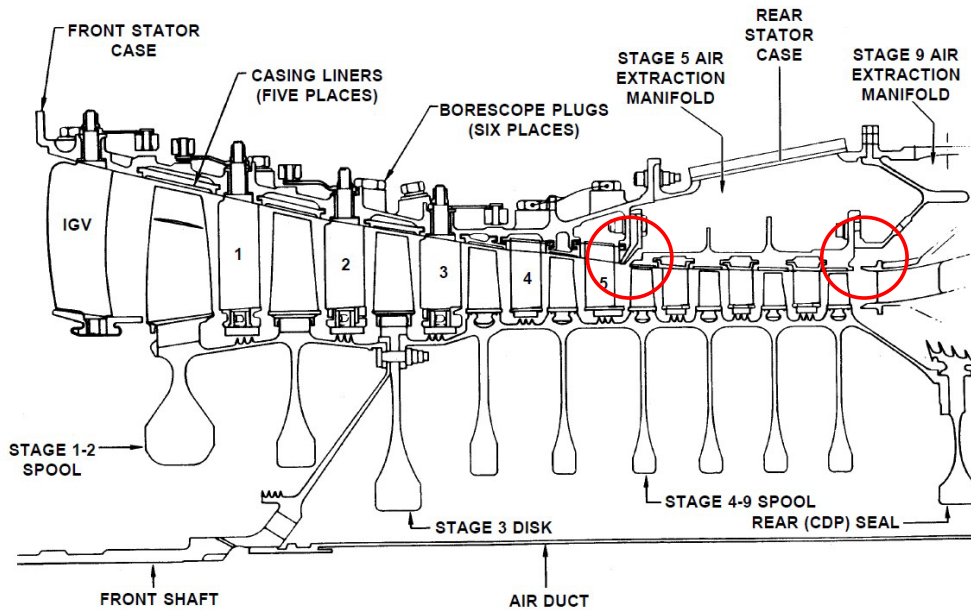


Figure 2.1: Bleed valve position CFM56 engine (Adapted from CFMI 2000)

The extraction of bleed air is necessary as the cabin has to be pressurized, as well as the supply of oxygen to the aircraft occupants. Except for the Boeing 787, this is done by means of the already compressed air from the high-pressure compressor of the engines. **Figure 2.2** shows the schematic diagram of the supply of the pressurized cabin with bleed air. The bleed air enters the air conditioning packs from the bleed ports. At this point the air is cooled down and moisture is removed. The air is then routed unfiltered into the mixer unit and distributed in the cabin.

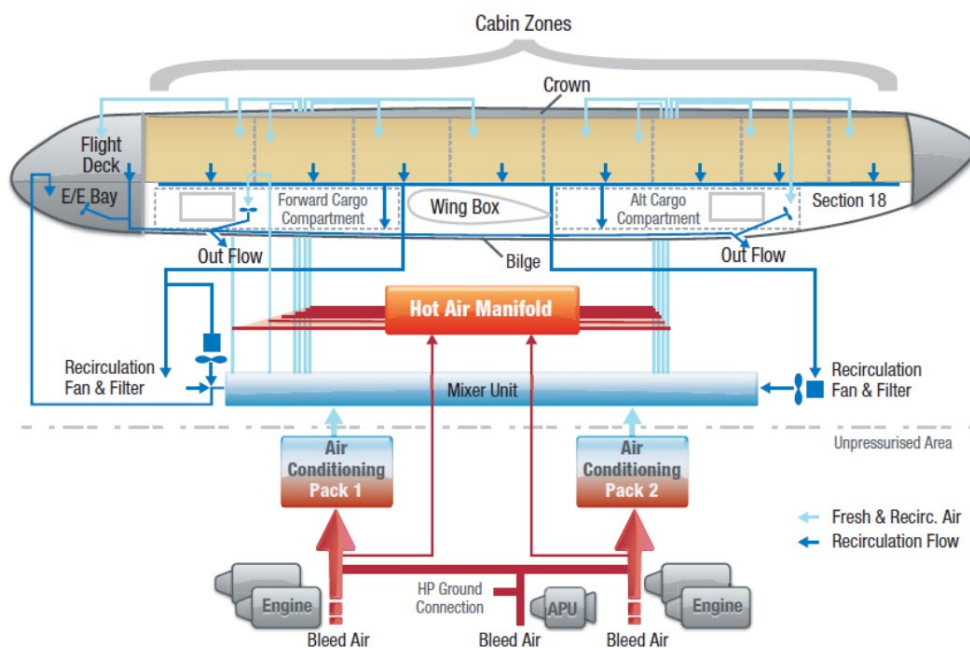
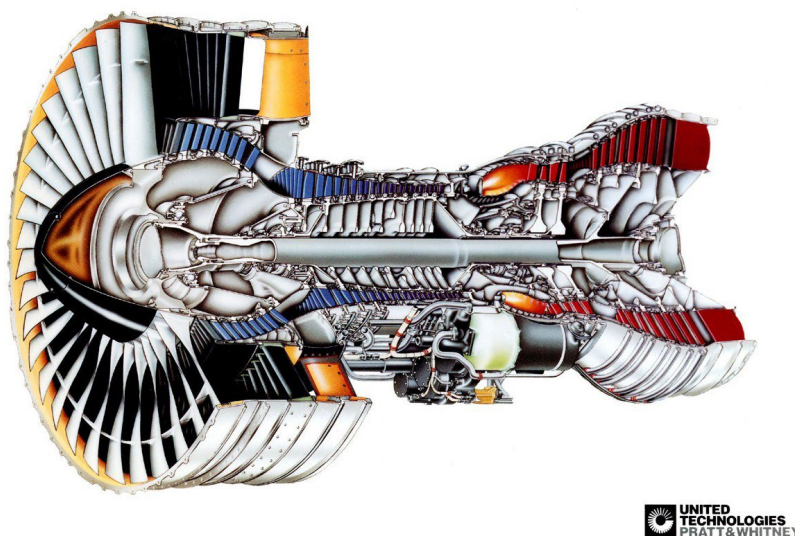


Figure 2.2: Typical air distribution (Lufthansa 2015)

The sources of contamination of the cabin air are known, as well as the causes. It is also clear how the contaminated air enters the cabin. One path that the contaminated air must also pass through to reach the bleed ports is from the bearing sumps to the abovementioned points in the high-pressure compressor. Engines are highly complex components, and it is particularly difficult to monitor airflows that are part of the external or internal air system.

The cooling and ventilation systems, active clearance control systems and the necessary compressor control systems belong to the category of external air systems. Internal air systems include cooling of components and seals, axial force balancing of rotors, and pressurization of bearing sumps. (Linke-Diesinger 2014)

Figure 2.3 shows a cutaway of the Pratt & Whitney PW4000-94 engine. Such pictures give a good impression of the engine design. The path of the main mass flow through the main components of the engine is clearly visible. Furthermore, in the front area some bearings can be seen.



©2014 UNITED TECHNOLOGIES CORPORATION – PRATT & WHITNEY DIVISION

Figure 2.3: Pratt & Whitney PW4000 engine (Pratt & Whitney 2014)

However, the **Figure 2.3** does not show in sufficient detail how the air for the bearing seal reaches the bearing sumps. A statement about the constructional design of the bearing sump cannot be made either. For this reason, the first part of Chapter 3 shows the construction of a bearing sump and the possible path of the contaminated air into the main gas flow of the engine by means of more detailed illustrations.

3 Possible Path of Lubricating Oil in an Aircraft Engine

To describe the possible path of the lubricating oil into the main gas flow of the engine, it is necessary to start where the lubricating oil no longer is forced to follow pipes and pumps. The main components of a lubricant system include the oil tank, pressure pump, bearing compartments and scavenge pump. The venting system also forms part of the system. This includes the de-oiler, which will be explained in Chapter 4. **Figure 3.1** shows a typical lubrication system with several bearing sumps within an engine. (Linke-Diesinger 2014)

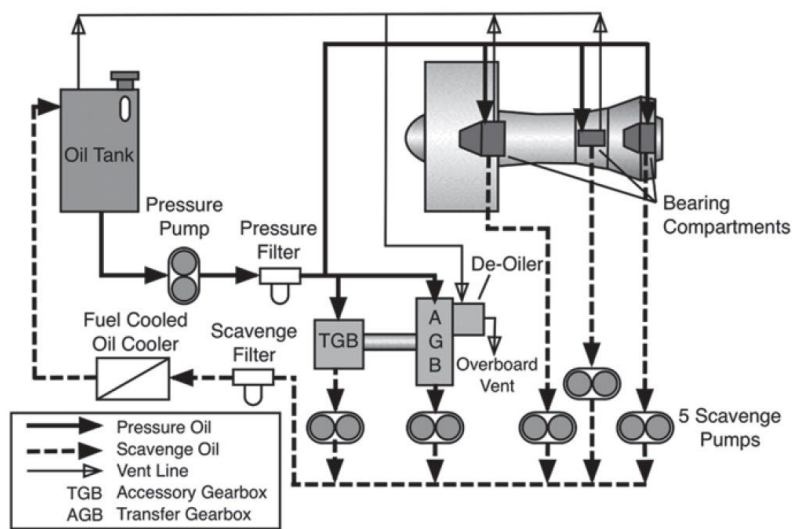


Figure 3.1: Lubrication system (Linke-Diesinger 2014)

The location where the lubricating oil does not follow the pipes or pumps is the bearing sump. A bearing sump contains one or more bearings that are supplied with lubricating oil by the lubricating oil system. The nozzles spray the lubricating oil onto certain areas of the bearing. The schematic diagram in **Figure 3.2** presents the lubrication system with a more detailed sump. Alternatively, the oil can also be fed through small channels in the bearing cages directly to the running surface of the bearings.

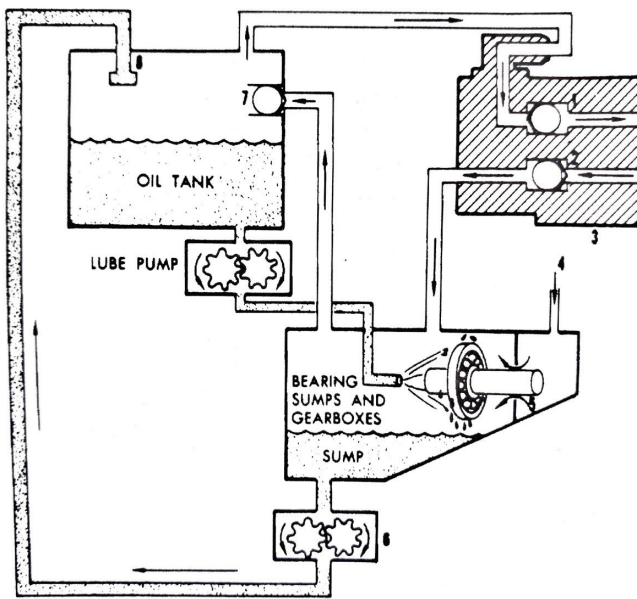


Figure 3.2: Bearing sump in lubrication system (Otis 1997)

Figure 3.2 demonstrates schematically that the sump only consists of one chamber and no seals are visible. If the sump shown in **Figure 3.2** is transferred to **Figure 3.3**, this is the inner sealing chamber. The second chamber is not included in **Figure 3.2**. For this reason, **Figure 3.3** shows the complete picture of a bearing sump. The bearing is enclosed by the first chamber. The oil accumulates at the bottom and is scavenged into the oil tank via the oil drain with the scavenge pumps. The air contaminated with oil (oil mist) is removed via the sump vent and fed to the de-oiler. The oil-cleaned air is led overboard. It should be mentioned that, in contrast to **Figure 3.3**, several bearings may be present in one bearing sump.

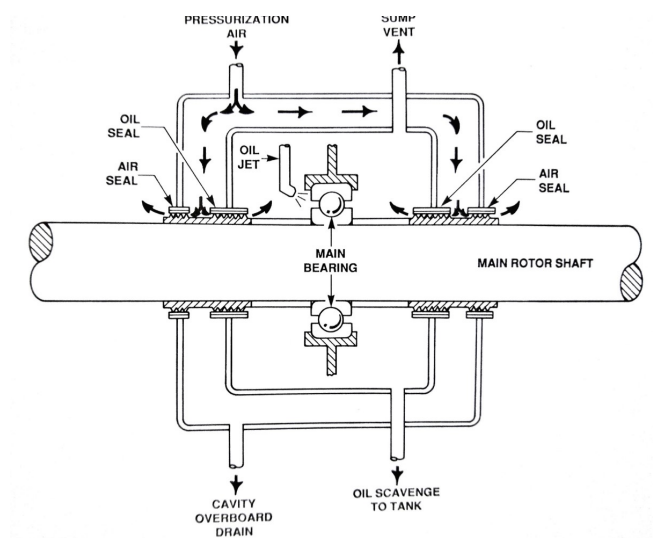


Figure 3.3: Typical bearing sump (Kroes 1994)

The oil seals of the first chamber can be seen in **Figure 3.3**. They prevent oil or oil mist from leaving the bearing chamber. The seal can be a carbon seal or a labyrinth seal. The first chamber is enclosed by another chamber. This chamber is filled with pressurized air. This air is extracted from the compressor at different compressor stages. This air flows through the seals into the inner chamber. This prevents polluted air from leak to the outer chamber. If the oil mist still succeeds to leave the first chamber, there is a possibility that the oil mist will also return to the main gas flow of the engine. If this point is upstream of the bleed valve to extract bleed air for the cabin, contaminated air may enter the cabin.

From the sump illustrations, it is not clear how an oil seal exactly looks like. To show illustrations of real engines presenting the structure of bearing sumps and the seals, the different types of seals are briefly described.

A labyrinth seal forms a non-contact seal. Thereby, characteristics create cross-sectional changes between a rotating part (shaft) and a stationary part. When a medium flows through the very small gap between the components, it then enters a groove between two labyrinth teeth. This process reduces the pressure of the medium due to the expansion. **Figure 3.4** shows a labyrinth seal. It should be noted that the permissible leakage flow is air that is fed into the bearing chamber from the main gas flow so that a volume flow, e.g. oil mist, towards the high-pressure side should be made more difficult. (Flitney 2014)

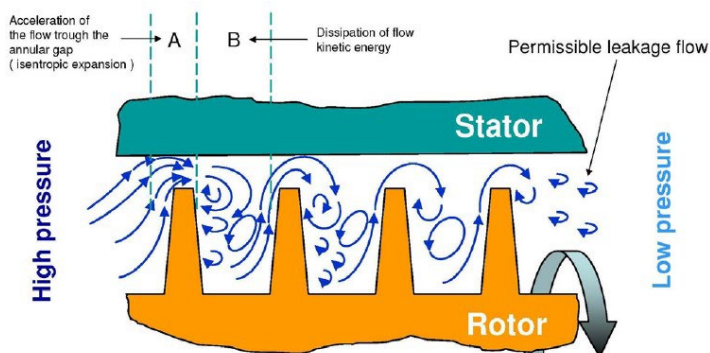


Figure 3.4: labyrinth seal with leakage flow (Flitney 2014)

There are different arrangements of the labyrinth seal to improve the sealing properties. Some of these arrangements can be seen in the following illustrations of the real engine types.

Another type of seal is the carbon face seal. They are also frequently used to seal bearing chambers. In contrast to the labyrinth seal, which is contactless, a carbon seal is a contact seal. **Figure 3.5** illustrates the design of a carbon seal. In a carbon seal, a static surface is pressed against a rotating surface by a spring and positive system pressure. The surfaces are wetted with a lubricant to increase the rotation speed and durability. (Flitney 2014)

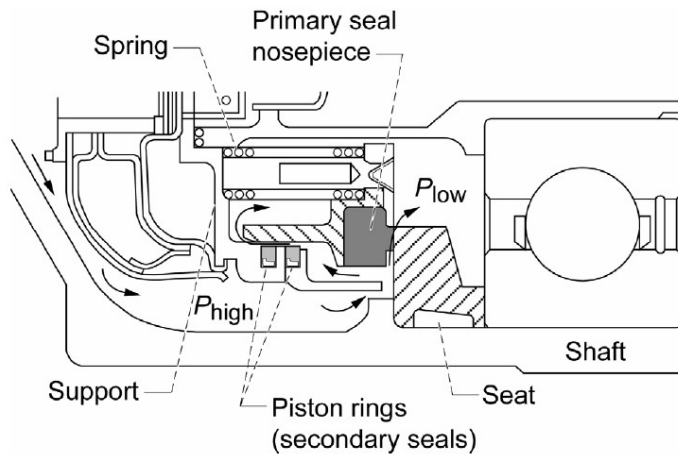


Figure 3.5: Carbon seal (Chupp 2006)

The sump illustrations (**Figure 3.2**, **Figure 3.3**) are only schematic representations. In the following it is shown based on illustrations of various engine types, how these chambers are constructed and how it might be possible for the oil mist to contaminate the main gas jet of the engine. The pictures used in the following section mainly show engine types that are rarely or not at all used in the current world fleet. However, for older engine models there are suitable pictures to illustrate the possible path of the air-oil mixture.

To get an idea of the possible air gas flow in an engine, **Figure 3.6** maps a cross-section of the United Technologies Pratt & Whitney JT8D Turbofan engine. This engine has three bearings that are located in front of the high pressure compressor (Treager 1995). The black arrows show the different paths of the air flowing through the engine. Between the last stage of the low-pressure compressor and the Vane compressed air is taken from the main gas stream (green marking). This air flows, among other ways, through the bearing sump. A major amount of the air is guided backwards by the low-pressure shaft and thus no longer encounters the main gas flow.

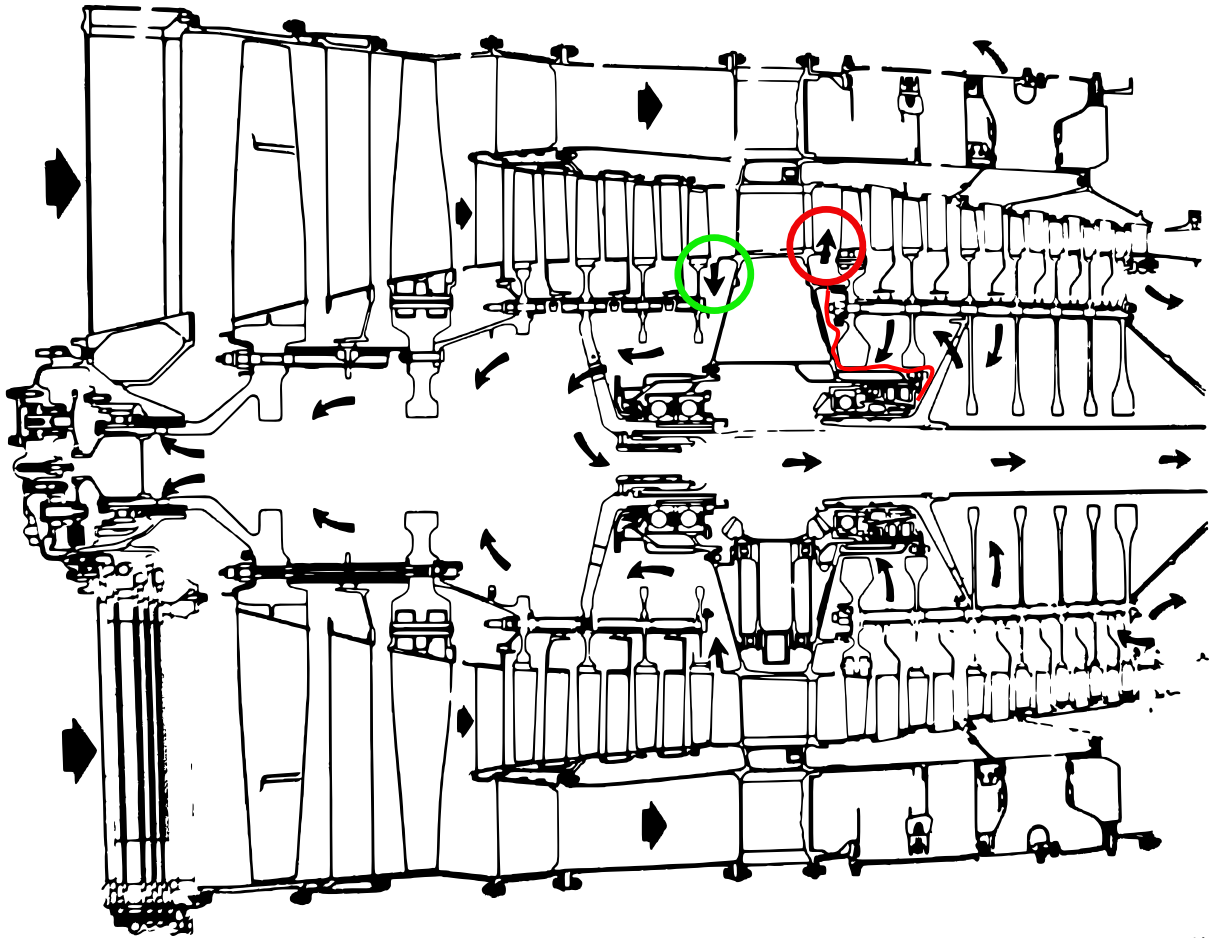


Figure 3.6: JT8D air path (adapted from Treager 1995)

It becomes clear that air can also flow back into the main gas flow coming from the bearing sump. The red path shows the possible path of the polluted air, starting from the sump. Here, the air returns to the main gas flow before the first stage of the high-pressure compressor. The bearings are depicted in more detail in **Figure 3.7**, so that the possible path of the oil-air mixture from the sump is clearly visible. This also reveals that several bearings are together in one sump. The bearing three (red circle) has a rear labyrinth seal. This indicates that it is a rear seal means that this seal is located downstream of the bearing in the gas flow direction. Sealing against the direction of gas flow is not necessary, as there is also a "wet" area where the oil is pumped out.

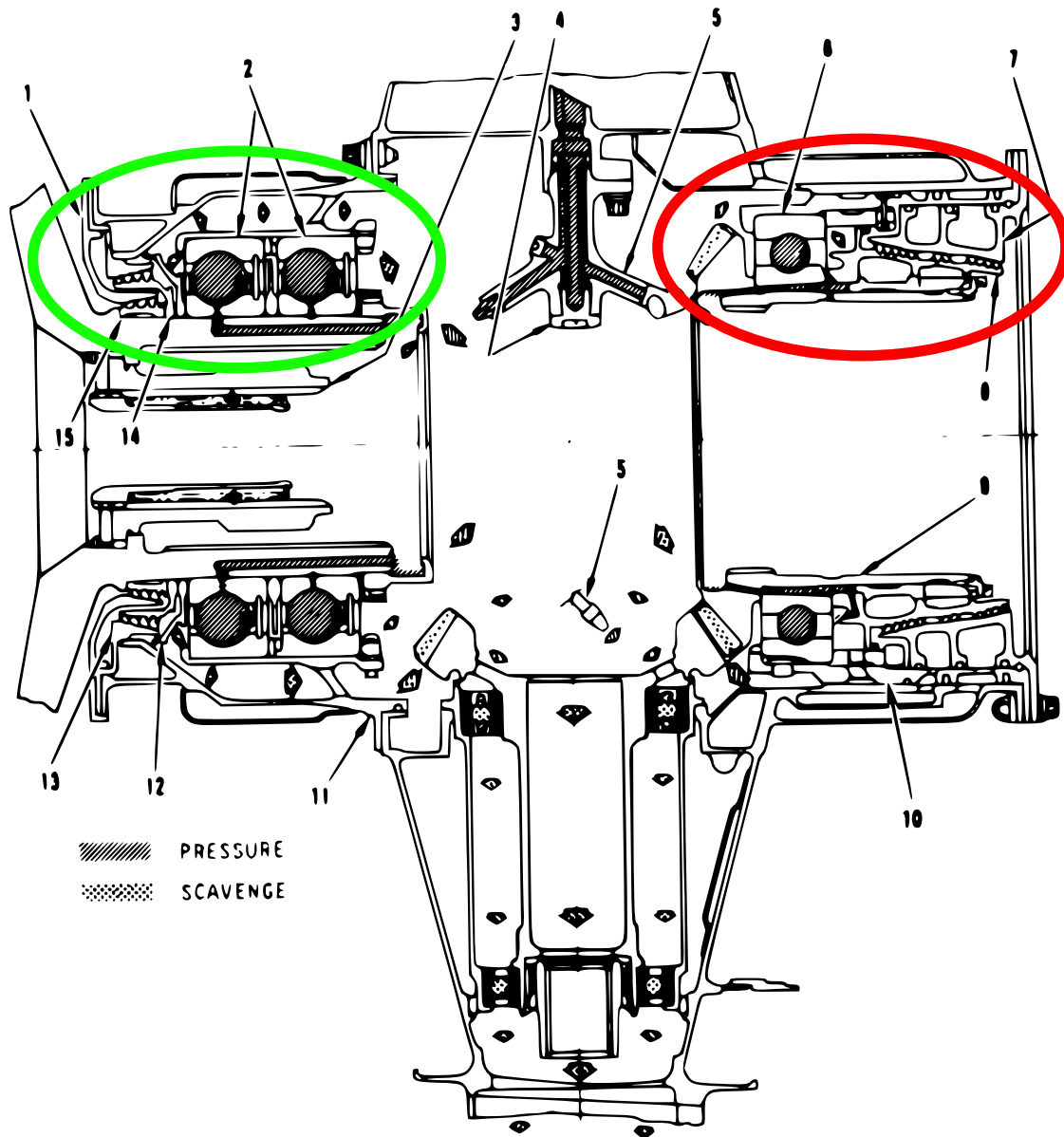


Figure 3.7: JT8D bearing sump (adapted from Treager 1995)

If the oil-air mixture has succeeded to flow through the labyrinth seal, this mixture is external to the sump seal and can follow the air flow (**Figure 3.6**) to the red mark and hence enter the main gas flow.

Figure 3.8 shows the structural precautions taken to prevent oil from escaping from the sump. The oil splashes against an oil baffle due to the centrifugal forces generated by the rotation of the shaft. This oil baffle gives the oil a new flow direction back towards the oil return pump. The oil baffle is attached to the compressor shaft and therefore rotates. For this reason it is necessary that there is a small gap between the oil baffle and the sump wall. The oil or oil-air mixture passing through this gap should then be stopped by two labyrinth seals. The mixture is only outside the sump when these seals have also been overcome.

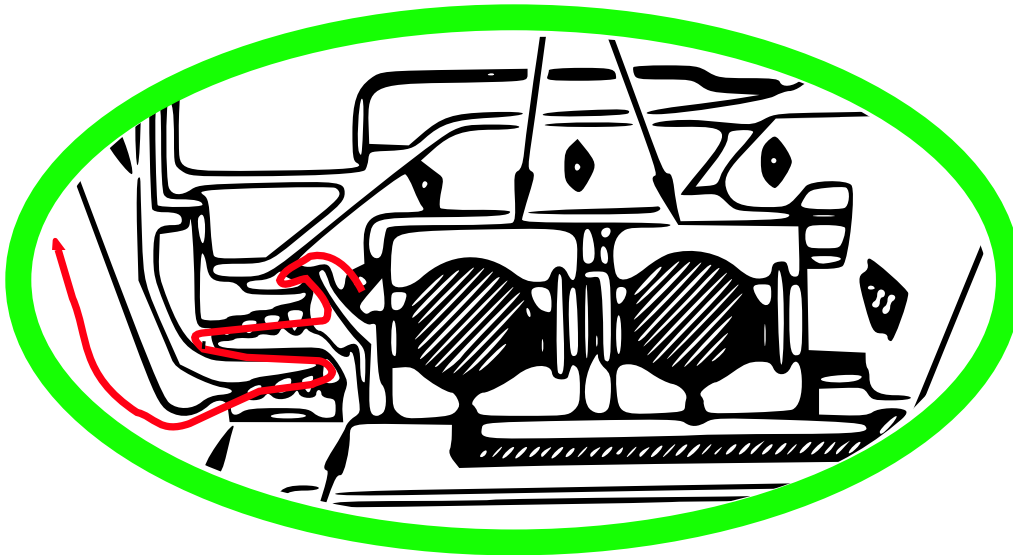


Figure 3.8: Detailed view of JT8D bearing (adapted from Treager 1995)

A bearing sump does not only contain one bearing. There can be several bearings in one sump. **Figure 3.9** shows the sump of the General Electric CF6-6, where the first ball bearing, the roller bearing number two, the ball bearing number three and the access to the gearbox part of the "A" sump are presented. (Otis 1997)

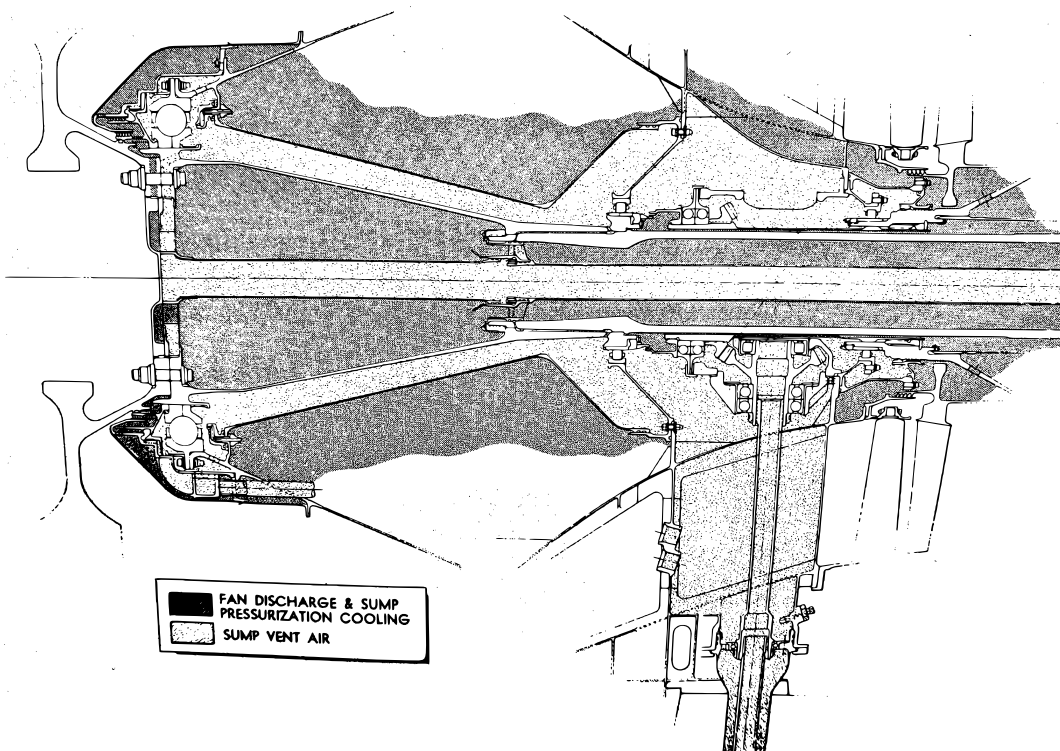


Figure 3.9: CF6 sump "A" (Otis 1997)

Figure 3.9 illustrates a good comparison between the schematic representation of the sump (**Figure 3.2**) and the design realization. The bearings shown in **Figure 3.9** are together in the slightly grey area. This is the "wet" sump.

At this point the lubricating oil is sprayed onto the bearings and the collected oil is pumped off in certain areas. The air-oil mixture is sucked off here. The slightly grey area is surrounded by a more contrasting, stronger grey. This is the second chamber in **Figure 3.2**, which is supplied with compressor air, so that ideally only air from the second chamber (strong grey) flows into the first chamber (light grey). (Otis 1997)

In the United Technologies Pratt & Whitney JT9D engine, it becomes visible that the first two bearings are housed together in a bearing sump. **Figure 3.10** shows the front sump of the JT9D engine.

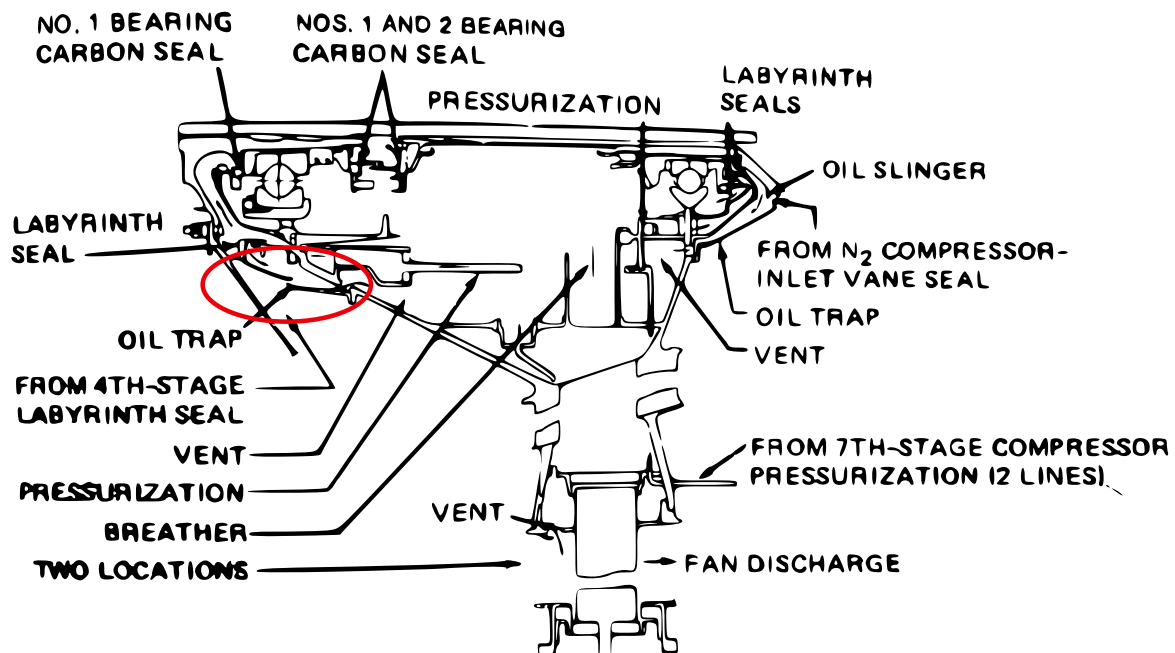


Figure 3.10: JT9D forward bearing (adapted from Kroes 1994)

The second chamber is charged with compressor air from the seventh stage. It should be mentioned that carbon seals can be seen here in the sump. The right ball bearing sits on the high-pressure shaft, the left ball bearing on the low-pressure shaft. The end of the high-pressure shaft is located in the sump. To create a seal here, carbon seals sit on the respective shaft ends, so that no oil gets between the shafts. Labyrinth seals and oil deflectors prevent the oil from leaving the inner chamber. To show the possible path of the oil mist into the main gas jet, the same position in the engine is shown in **Figure 3.11** as in **Figure 3.10**. However, in **Figure 3.11** the bearing is not depicted. To find the connection between both figures, the identical oil trap is highlighted in both figures.

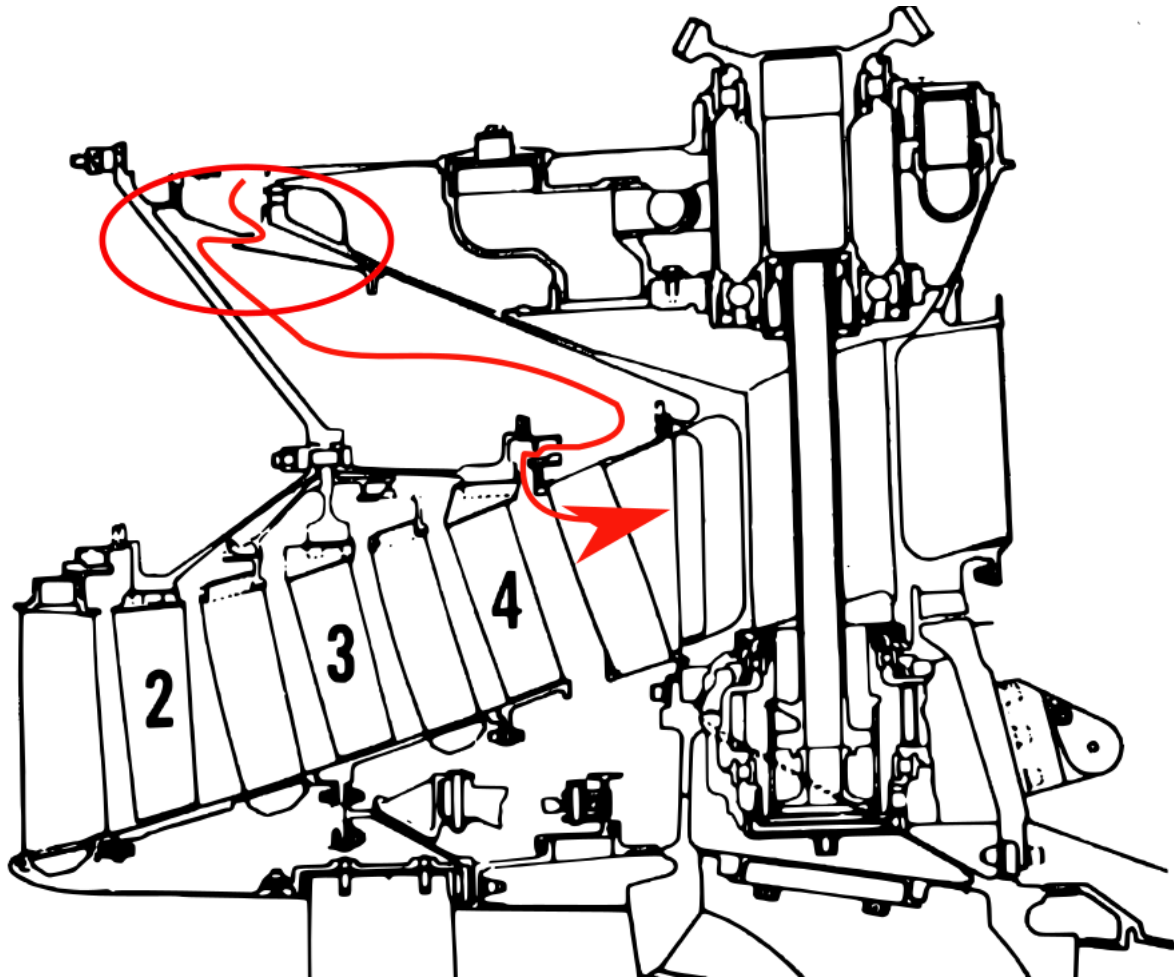


Figure 3.11: JT9D main gas stream (adapted from Kroes 1994)

Figure 3.10 displays that air is extracted at compressor stage 4 and passed through the oil trap. If the air-gas mixture has succeeded in flowing through all the seals and also against the direction of flow at the oil trap, it may also be able to pass through the last labyrinth seal between compressor blade 4 and the stator.

Finally, **Figure 3.12** shows bearing number two of the General Electric T58 engine. Two labyrinth seals prevent the air-oil mixture from leaving the sump. The first labyrinth seal is attached to the shaft and thus rotates. The air is now forced to follow an "S-curve" in order to pass through a second labyrinth seal. This seal is static and therefore does not rotate. A last labyrinth seal is located on the last rotor stage. If the mixture is able to overcome this seal, enters in the main gas flow of the engine.

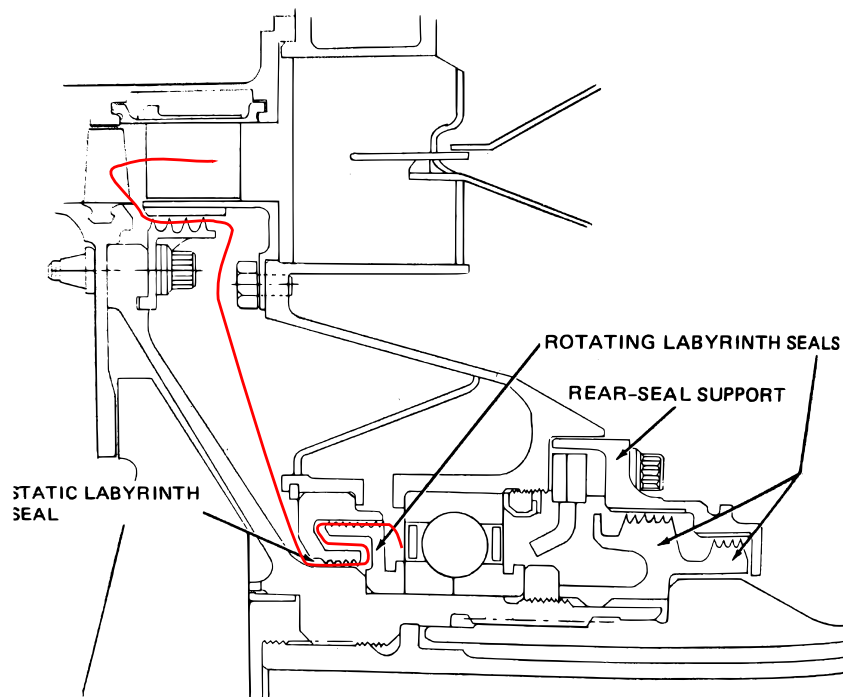


Figure 3.12: Bearing two of the T58 jet engine (adapted from Treager 1995)

It turns out that there are quite plausible paths that the oil-air mixture could follow to enter the main gas flow of the engine. However, this requires some assumptions. These include that the oil-air mixture can leave the first chamber despite the pressure gradient between the first and second chamber. It will then be able to continue to move against the air flow from the direction of the compressor nozzles and continue to overcome seals.

4 Volume and Mass Flow Rates in the Bearing Chamber and Breather

For the best possible sealing of the bearing sump, air is directed through the seals in the direction of the bearings. A complex two-phase mixture of air and oil is created in the bearing chamber. (Kurz 2012) **Figure 4.1** presents a sectional view of the bearing chamber and illustrates the generation of these phases. The oil is scavenged into the oil tank by the scavenge pump. At this point, air is also pumped out which is separated from the oil in the oil tank by another breather. The oil-contaminated air in the bearing chamber is led to the breather via the vent line.

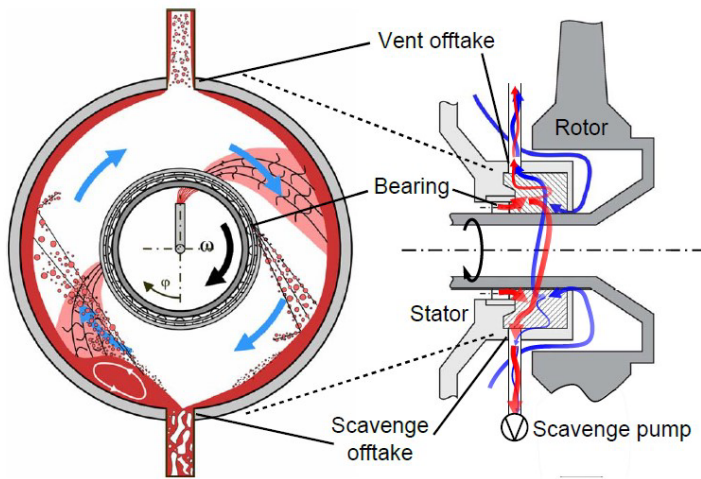


Figure 4.1: Bearing chamber two-phase flow (Kurz 2012)

There are two types of breather to separate the oil from the air. If it is a bearing chamber as shown in **Figure 4.1**, the oil-air mixture flows into an air centrifuge. This is called a de-oiler or de-aerator and is illustrated in **Figure 4.2** (Linke-Diesinger 2014). The oil mist has passed into a chamber in which a rotor rotates. This rotor contains a porous material. Due to the pressure gradient between the environment and the pressure in the chamber, the air flows through the porous material. Large oil droplets have already been sprayed against the chamber wall and separated from the air due to the rotational flow in the chamber. The small droplets then remain adhered to the porous material and are guided back into the chamber. In this way, almost only pure air reaches the environment via the rotor's shaft. (Cordes 2017)

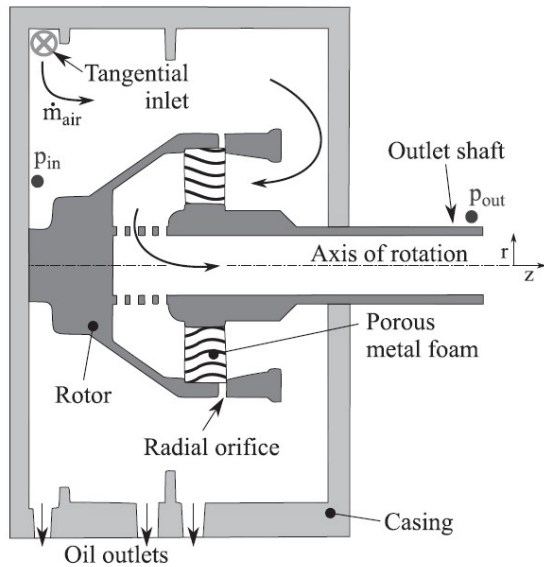


Figure 4.2: De-aerator, de-oiler (Cordes 2017)

Another option is to vent the air from the bearing chamber via the low-pressure shaft of the engine. The engine manufacturers CFM and GE have taken this design principle. This breather type is known as an air/oil separator. (Linke-Diesinger 2014) For this type, the rotating shaft is provided with holes, which are also filled with a porous material. The principle is similar to that of the de-oiler, except for the fact that the low-pressure shaft in this variant is the rotating component. **Figure 4.3** shows an air/oil separator of a CFM 56-5A engine, marked with a red circle. It is the front sump, in which the first three bearings are located.

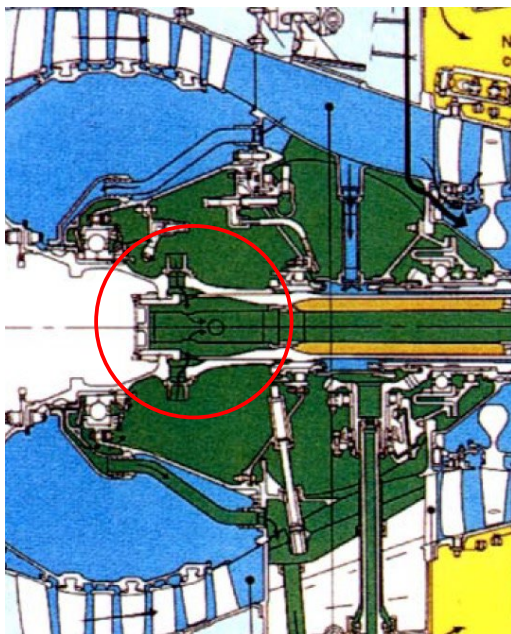


Figure 4.3: Air/Oil Separator CFM56-5A (adapted from CFMI 2000)

For a further consideration of assumptions of values of the contaminated air entering the cabin via the bleed air, mass and volume flows in a bearing chamber are presented in the following section. This provides a basis for comparison as to whether the assumptions are realistic in their magnitude. In addition, information on the mass and volume flows of the lubricating oil is given, so that an impression can be gained of how much oil flows through the breather and thus has to be filtered out of the contaminated air. The oil consumption of an engine depends largely on the efficiency of the breather, which separates the oil from the air and feeds it back into the oil tank. However, the efficiency of a breather has no effect on contaminated cabin air, because the cleaned sealing air is not returned to the main gas flow of the engine. Nevertheless, it is possible to gain an impression of the importance of efficiency in the oil consumption of an engine.

Figure 4.4 displays the schematic structure of a bearing chamber, as well as the researched dimensions and volume flows. In addition, **Table 4.1** displays the numbered arrows.

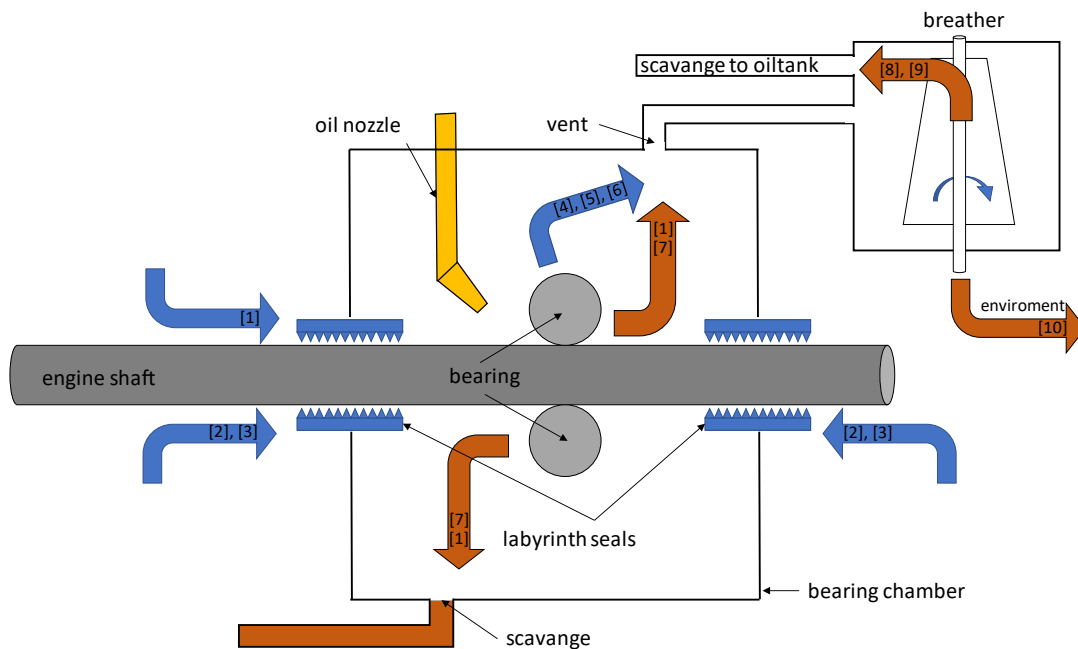


Figure 4.4: Volume/mass flow bearing chamber

Table 4.1: Conclusion of values from **Figure 4.4**

Number	Value	Description	Reference
[1]	15 g/s 40% / 60%	Air mass flow bearing chamber Vent/scavenge oil mass flow	(Farrall 2006)
[2]	5 g/s ... 20 g/s	Air mass flow bearing chamber	(Busam 2000)
[3]	23 g/s ... 33 g/s	Air mass flow bearing chamber	(Aidarinis 2011)
[4]	45 g/s	Air mass flow separator	(Eastwick 2006)
[5]	60 g/s ... 100 g/s	Air mass flow separator	(Lu 2014)
[6]	50 g/s	Air mass flow separator	(Care 1999)
[7]	21% ... 56%	Scavenge efficiency oil volume flow	(Kurz 2012)
[8]	at least > 80%	Breather efficiency	(Jingyu 2016)
[9]	99.98%	Breather efficiency	(Willenborg 2006)
[10]	0.1 l/h ... 0.5 l/h	Oil volume flow to environment (CFM 56)	(Linke-Diesinger 2014)

The air mass flows differ in their magnitude, in some cases remarkably. Most of the data contains values that were used in tests to investigate processes in a bearing chamber or breather. For this reason, some of the values are given in ranges, since the tests were carried out with different parameters. Nevertheless, the values are based on real engine conditions.

"Air and oil flows are arranged in the same way as in the real engine." (Busam 2000)

The efficiency of the scavenge process of (Kurz 2012) refers to a certain design arrangement of the vent and scavenge lines. It is a basic arrangement; the pipes are on the same height as the inner wall of the storage chambers. Changes to the design will improve efficiency so that more oil is discharged through the scavenge line. However, this is not part of this consideration.

The breather efficiency of (Jingyu 2016), refers to an axial breather, i.e. an air/oil separator, that is used in CFM engines. Considerably higher efficiencies are already achieved. This is also demonstrated in the test conducted by (Jingyu 2016), the efficiency is 99.6%. Despite this, the statement of an efficiency of 80% is relevant and can be of importance when considering the statement of (Linke-Diesinger 2014). This is also an indication of a CFM engine.

It should be noted that for comparative calculations or estimations of resulting values from **Table 4.1**, the physical properties of air must be considered. Above all, the pressure and the resulting density of the sealing air differ at the sources.

5 Evaluation of Design Parameters

Scholz (Scholz 2017) developed the Equation (5.1), allowing an estimation of the amount of lubricating oil in the cabin air. The mass of the oil is set in relation to the volume of the cabin air $m_{oil,cab}/V_{cab}$.

$$\frac{m_{oil,cab}}{V_{cab}} = \frac{\dot{m}_{oil} \cdot x_{bear,up} \cdot x_{seal}}{S_{eng} \cdot n_{eng} \cdot M_{CR} \cdot a(h_{CR})} \cdot \frac{\rho_{cab}}{\rho_{CR}} \cdot (\mu + 1) \quad (5.1)$$

Furthermore, an exemplary calculation (5.2) was carried out using the CFM56 engine. This calculation is shown below.

$$\frac{m_{oil,cab}}{V_{cab}} = \frac{0,163 \frac{g}{s} \cdot 0,6 \cdot 0,01}{2,35 \text{ m}^2 \cdot 2 \cdot 0,76 \frac{m}{s}} \cdot \frac{0,963 \frac{kg}{m^3}}{0,364 \frac{kg}{m^3}} \cdot (5,7 + 1) = 17 \frac{\mu g}{m^3} \quad (5.2)$$

The values in the denominator from (5.1) are engine- and aircraft-related. They vary when considering different aircraft engine configurations and are not examined in detail within this study. The mass flow \dot{m}_{oil} depends on the engine. This parameter defines the oil consumption of the engine. It is difficult to find reliable values for oil consumptions of current engine types. In (Scholz 2018) oil consumption data is collected from forums. In addition, **Table 5.1** displays the oil consumption of some engine types. It should be noted that the data only represent an approximate value. Within an engine model, the consumption values differ for the different engine series. The oil consumption of the engine types even changes over the years, for example due to design modifications. For the conversion into a volume flow rate, the lubricating oil Mobil Jet Oil II with a density of 1.0035 kg/l was used for all engines.

Table 5.1: Oil consumption for different engine types

Engine	Value	Reference	Converted in l/h
JT8D	1360 g/h	(Kroes 1994)	1,35
JT9D	1360 g/h		1,35
JT15D	227 g/h		0,23
CF6-6	1360 g/h		1,35
CF6-50	1360 g/h		1,35
CFM56	0,3 qts/h	(LTT 1999)	0,35
	0,1-0,5 l/h	(Linke-Diesinger 2014)	-
TFE731	408 g/h	(Kroes 1994)	0,41
RB211	907 g/h		0,90
GE90	0,34 l/h	(Transportation Safety Board of Canada 2012)	-
V2500	0,3 qts/h	(Japan Transport Safety Board 2012)	0,35

To get an impression of the oil concentration in the cabin air, further values of different engine types are evaluated in addition to the oil concentration from (5.2). The calculation is

concentrated on engines for those the bearing configuration could be determined unambiguously. These oil concentrations can be found in **Table 5.2**, calculated for some engine types and aircraft configurations. For a first impression of the oil in the cabin air, certain parameters in the equations are kept constant for all engine types; these are based on the values of (Scholz 2017). These constant parameters depend on the aircraft type, except for x_{seal} . The oil mass flow \dot{m}_{oil} is calculated with the density of the Mobil Jet Oil II lubricating oil.

Table 5.2: Calculation of the Oil Concentration in the Cabin

Parameter	CF34	V2500	CFM56	PW4000	GE90
\dot{V}_{oil}	0,2 qts/h ^a	0,28 qts/h ^a	0,3 qts/h ^b	0,5 qts/h ^a	0,34 l/h ^c
\dot{m}_{oil}	0,1115 g/s	0,1516 g/s	0,1673 g/s	0,5241 g/s	0,1895 g/s
$x_{bear,up}$	3/5 ^d	3/5 ^e	3/5 ^b	3/5 ^f	4/6 ^g
x_{seal}			0,01 ^h		
S_{eng}	1,42 m ^{2 i}	2,06 m ^{2 j}	2,35 m ^{2 b}	4,48 m ^{2 f}	8,3 m ^{2 k}
n_{eng}	2 ^l	2 ^l	2 ^l	4 ^l	2 ^l
M_{CR}	0,78 ^l	0,78 ^l	0,76 ^l	0,85 ^l	0,84 ^l
$a(h_{CR})$			295 m/s ^h		
ρ_{cab}			0,963 kg/m ^{3 h}		
ρ_{CR}			0,364 kg/m ^{3 h}		
μ	5,4 ⁱ	4,5 ^j	5,7 ^b	4,8 ^f	9 ^k
$\frac{\dot{m}_{oil,cab}}{V_{cab}}$	17,3 $\frac{\mu g}{m^3}$	14,4 $\frac{\mu g}{m^3}$	16,9 $\frac{\mu g}{m^3}$	10,7 $\frac{\mu g}{m^3}$	8 $\frac{\mu g}{m^3}$

^a (Scholz 2018), ^b (LTT 1999), ^c (Transportation Safety Board of Canada 2012), ^d (SmartCockpit 2020),

^e (MTU Maintenance 2020), ^f (Sumner 1997), ^g (Aviation 2016), ^h (Scholz 2017), ⁱ (GE Aviation 2010),

^j (IAE 2016), ^k (MTU Aero 2020), ^l These parameters may vary due to engine/aircraft configuration.

The lowest oil concentration in the cabin was determined based on the GE90 parameters. The maximum value, more than two times higher than the minimum value, was calculated with the CF34 engine parameters.

A closer look at the parameters shows that compared to the CF34 parameters, the engine data of the GE90 engine generally has a higher value. The ratio between the parameters is slightly above 1, apart from the engine intake area. Here, the ratio is 5.8 times larger than the first one, which is the main reason for the difference of the results. A high bypass ratio μ results in an increased oil concentration in the cabin since less air flows through the core engine and thus the oil is concentrated in reduced air volumes. An engine optimized according to (5.1) with respect to the oil concentration in the cabin thus has a large fan diameter, with all air streaming through the core engine. It should be mentioned that the assumption is valid by which the oil is distributed consistent in the main gas flow and by which this concentration is also found in the cabin air (Scholz 2017).

In order to estimate the oil in the cabin air, an assumption has to be made on how much oil leaks out of the bearing sump. On the basis of oil consumption, a percentage assumption x_{seal} is made as to how much oil passes through the seals into the main gas flow. Due to the fact that only oil can enter the cabin when entering the main gas flow before the bleed air is extracted, a ratio $x_{bear,up}$ is calculated in (5.3). This ratio is calculated from bearings before the bleed air extraction to the total number of bearings in the engine.

$$x_{bear,up} = \frac{n_{bear,up}}{n_{bear}} \quad (5.3)$$

This results in the oil mass flow $\dot{m}_{oil,comp}$ into the cabin to

$$\dot{m}_{oil,comp} = \dot{m}_{oil} x_{bear,up} x_{seal}. \quad (5.4)$$

It becomes clear that the oil present in the cabin air depends on the number of bearings and their position. Thus, the assumption is made that one bearing is responsible for a certain amount of oil consumption. In Chapter 3, it can be seen that several bearings are located in one sump. To illustrate the allocation of the bearings in the sump, **Figure 5.1** shows the bearing distribution in a CFM56 engine, which is also the basis of the calculation from (5.2).

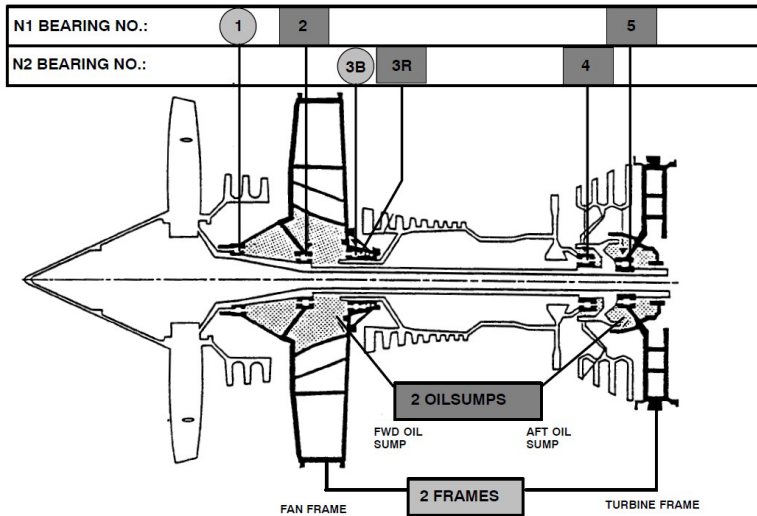


Figure 5.1: Bearing sump CFM56 (LTT 1999)

There are three bearings in the front oil sump. If theoretically a further bearing is added to the front oil sump, the mass flow of oil would increase after (5.3) and as a result in (5.4). However, the sealing of the sump is basically the component responsible for the oil leakage from the sump and thus for the contamination of the cabin air. A further bearing would not necessarily have to change the sump seal; but it does have an influence on the oil consumption according to (5.4). For this reason, a new approach would be to determine the oil

consumption depending on possible ways out of the sump. **Figure 5.2** shows the front bearing sump of the CFM56 engine. The arrows visualize the path of the sealing air to the seals.

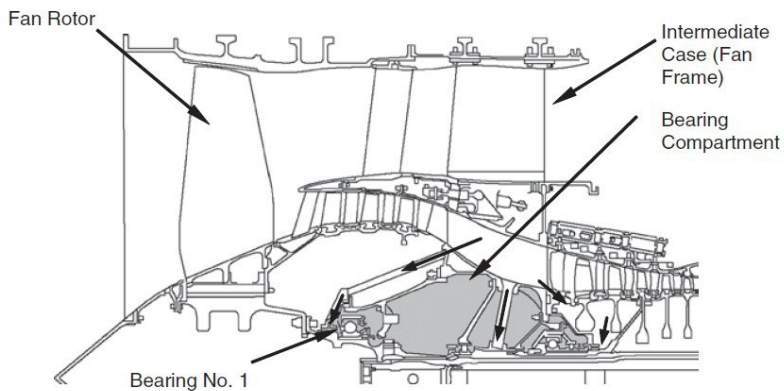


Figure 5.2: Front bearing sump CFM56 (Linke-Diesinger 2014)

The sealing air flows through the seals into the bearing chamber from three directions. **Figure 5.3** shows a more detailed view of the bearing sump seen in **Figure 5.2**. Indicated in blue is the oil supply of the two front bearings. Green indicates the vent air, which is separated from the oil in the front sump by an Air/Oil Separator. The green vertical bar is no real path of the vent air in the engine.

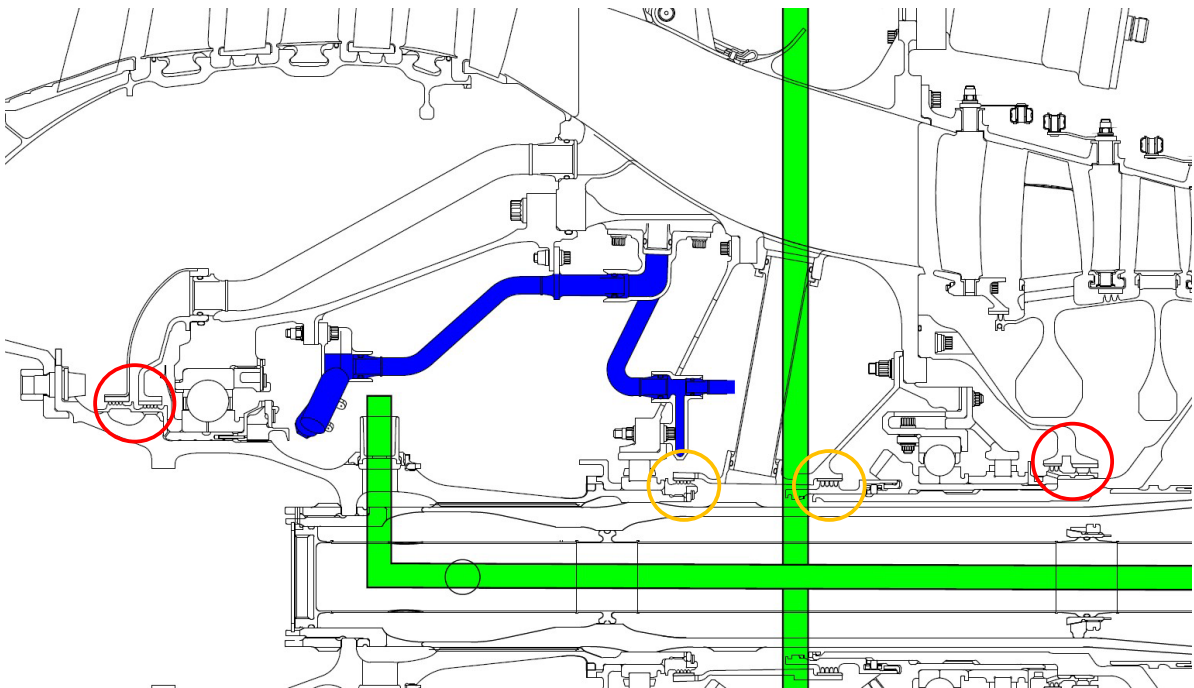


Figure 5.3: Detailed front sump CFM56 (adapted from <https://de.scribd.com/document/230227151/CFM56-7B-Lube-System>)

The bearing seals framed in red form the beginning and end of the front bearing sump. Between bearing two and three there are two more orange marked seals. Thus, there are four ways that the contaminated air can leak out of the sump. The challenge, however, is to select a ratio that can properly represent the proportion of oil that enters the main gas stream before the bleed air is extracted. One possibility would be to determine a ratio, similar to the ratio of the bearing arrangement, with the number of possible paths that the contaminated air can take from the sumps. Despite that, it is difficult to determine these paths, especially in the rear sump, using the example of the CFM56 engine with the available figures.

In summary, it can be said that the consideration of the number of sump sealings should be included in the calculation, but this is only possible when the leakage performance of the individual seals is known. With the data of the mass or volume flow of the sealing air shown in Chapter 4, it is possible to determine as to how much oil escapes from the respective number of seals. Independent from the number of bearings in the sump, there is also more oil mist in the front sump of the engine, since the oil mist from the oil tank and the transfer gearbox and accessory gearbox is also fed into the front sump (CFMI 2000).

6 Summary and Conclusions

The cause or source of a CACE is generally known. Since it is not possible to develop a leakproof seal, there will always be oil leaking out of the bearing sump. For this reason, the Chapter 2 shows how the oil can get into the main gas flow. One possible path from the bearing chamber into the main gas flow is demonstrated. Detailed pictures of real engine types are used to show how oil drops can pass through the bearing seals. The focus is not on the leakage path within a specific type of seal, but rather, from a macroscopic point of view, on overcoming all seals and the path from the shaft to the main gas flow. It is shown at which position the air in the main gas path of the engine was tapped to be led into the bearing chamber as sealing air. On this basis, it is assumed that the oil can also take the same path in the opposite direction. Furthermore, the real engine drawings are used to demonstrate how a bearing sump is constructed. It becomes clear that several bearings are located in one bearing sump.

After the study of real bearing chambers of engines, volume and mass flows in a bearing chamber are taken into account. A bearing chamber has always a breather, which removes oil from the sealing air. The efficiency of this breather is the main reason for the oil consumption of an engine, that is why the breather is considered for the analysis. It becomes clear to which magnitude sealing air enters the bearing chamber.

The reason for considering the design of bearing sump, breather and operating conditions in a bearing sump is to provide a basis for applying the presented equation for calculating oil in the aircraft cabin. The operating conditions are not covered in the following discussion of the equation. These are to be used as a basis if, by modifying the equation, other parameters have an influence on the oil concentration in the cabin air.

For a further implementation of this approach, it is necessary to determine detailed images of engine models. This is especially challenging for illustrations of up-to-date engine models. In addition, a literature search should be conducted to determine the oil leakage performance of the seals. It should be noted that there are values for the leakage performance of seals, but these are usually values for the required sealing air, which is guided through the seals into the bearing chamber. If these basics are available, a good estimation is possible to determine the oil content in the cabin air depending on the design of the engine bearings and oil seals.

List of References

- AIDARINIS, J., MISSIRLIS, D., YAKINTHOS, K., and GOULAS, A., 2011. CFD Modeling and LDA Measurements for the Air-Flow in an Aero Engine Front Bearing Chamber. In: *ASME. J. Eng. Gas Turbine Power*, vol. 133, no 8, pp. 082504.
Available from: <https://doi.org/10.1115/1.4002830>
- AVIATION, 2016. Internet forum. *Aviation Stack Exchange* [viewed 22 March 2020].
Available from: <https://bit.ly/2UrSIrd>
Archived at: <https://perma.cc/ATC2-SN2J>
- BUSAM, S., GLAHN, A., and WITTIG, S., 2000. Internal Bearing Chamber Wall Heat Transfer as a Function of Operating Conditions and Chamber Geometry. In: *ASME. J. Eng. Gas Turbine Power*. vol. 122, no. 2, pp. 314-320.
Available from: <https://doi.org/10.1115/1.483209> (Open Access)
- CARE, Ian, S., EASTWICK, C. N., HIBBERD, S., SIMMONS, K., and WANG, Y., 1999. CFD Computation of Air-Oil Separation in an Engine Breather. In: *IMEchE conference on CFD Developments and future trends*, London.
Available from: <https://bit.ly/2UUIvoR> (Open Access)
Archived at: <https://perma.cc/J7GG-FCAZ>
- CFMI, 2000. *Training Manual CFM56-5A Engine Systems*
Available from: <https://bit.ly/38wN2C7> (Open Access)
Archived at: <https://perma.cc/47PA-PLF2>
- CHILDS, Peter RN., 2019. Aircraft Cabin Air Supply and the Internal Air System. In: *Journal of Health and Pollution*, vol. 9, no. 24, pp. 17-21.
Available from: <http://doi.org/10.5281/zenodo.3605028> (Open Access)
- CHUPP, Raymond E., et al. 2006. Sealing in Turbomachinery. In: *NASA/TM-2006-214341*. Ohio: National Aeronautics Space Administration.
Available from: <https://go.nasa.gov/2UXYoL9> (Open Access)
Archived at: <https://perma.cc/QXY6-4NUT>
- CORDES, A., et al, 2017. Experimental Study of Pressure Lost in Aero-Engine Air-Oil Separators. In: *The Aeronautical Journal*, vol. 121, no. 1242, pp. 1147-1161.
Available from: <https://doi.org/10.1017/aer.2017.41>
Open Access at: <https://bit.ly/2u18H67>
Archived at: <https://perma.cc/82GC-MZKD>

- DAY, Gregory A., 2015. *Aircraft Cabin Bleed Air Contaminants: A Review*. Oklahoma City: FAA Civil Aerospace Medical Institute
 Open Access at: <https://bit.ly/2SmaKdq>
 Archived at: <https://perma.cc/GYS7-SLA5>
- EASTWICK, C. N., SIMMONS, K., WANG, Y., and HIBBERD, S., 2006. Study of Aero-Engine Oil-Air Separator. In: *Institution of Mechanical Engineers, Parts A: Journal of Power and Energy*, vol 220, no, 7, pp. 707-717.
 Available from: <https://doi.org/10.1243/09576509JPE116>
 Open Access at: <https://bit.ly/2UUTDSJ>
 Archived at: <https://perma.cc/NC8T-XNXN>
- FARRAL, M., HIBBERD, S., SIMMONS, K., and GIDDINGS, D., 2006. Prediction of Air/Oil Exit Flows in Commercial Aero-Engine Bearing Chamber. In: *Institution of Mechanical Engineers, Parts G: Journal of Aerospace Engineering*, vol. 220, no. 3, pp. 197-202.
 Available from: <https://doi.org/10.1243/09544100JAERO40>
- FLITNEY, Robert K., 2014. A Description of the Types of High Speed Rotary Shaft Seals in Gas Turbines Engines and the Implications for Cabin Air Quality. In: *Journal of Biological Physics and Chemistry*, vol. 14, no. 4, pp. 85-89.
 Available from: <https://bit.ly/2Uc8hnG> (Open Access)
 Archived at: <https://perma.cc/9952-QDRC>
- GE AVIATION, 2010. *CF34-10E turbofan propulsion system*.
 Available from: <https://www.geaviation.com/sites/default/files/datasheet-CF34-10E.pdf>
 Archived at: <https://perma.cc/3CLU-VKFH>
- IAE, International Aero Engines, 2016. *V2500 The Engine of Choice*.
 Available from: http://www.i-a-e.com/pdf/V2500_Product_Card_060716.pdf
 Archived at: <https://perma.cc/H8JX-XTT4>
- JINGYU, Zhao., ZHENXIA, Liu, and GUOZHE, Ren, 2015. The Design and Performance Evaluation of Axial Ventilator with Honeycomb in the Turbofan Engine Lubrication System. In: *Institution of Mechanical Engineers, Parts G: Journal of Aerospace Engineering*, vol. 230, no. 8, pp. 1397-1408.
 Available from: <https://doi.org/10.1177/0954410015611151>
- KROES, Michael, and WILD, Thomas W., 1994. *Aircraft Powerplants*. 7th ed., New York: MC Graw Hill Companies.

- KURZ, Wolfram, DULLENKOPF, Klaus, and BAUER, Hans-Jörg, 2012. Influence on the Oil Split Between the Offtakes of an Aero-Engine Bearing Chamber. In: *ASME Turbo Expo 2012: Turbine Technical Conference and Exposition*, vol. 220, no. 3, pp. 197-202.
Available from: <https://doi.org/10.1115/GT2012-69412>
- LINKE-DIESINGER, Andreas, 2014. *Systeme von Turbofan-Triebwerken*. Berlin Heidelberg: Springer Vieweg,
- LU, Ya Guo, and HU, Jian Ping, 2014. Numerical Simulation for Air/Oil Separator of Aero-Engine. In: *Applied Mechanics and Materials*, vol. 510, pp. 197-201.
Available from: <https://doi.org/10.4028/www.scientific.net/AMM.510.197>
Open Access at: <https://bit.ly/2JbUbfQ>
Archived at: <https://perma.cc/FN58-ZA2T>
- LUFTHANSA, 2015. *Lufthansa Spotlight #2: Kabinenluft*.
Available from: <https://bit.ly/374IKQz>
Archived at: <https://perma.cc/W242-G4BM>
- LTT, Lufthansa Technical Training, 1999. *Training Manual A319/ A320/ A321 ATA 71-80 Engine CFM 56-5A*. Hamburg
Available from: <https://bit.ly/37yk9UL>
Archived at: <https://perma.cc/YVT9-QWM9>
- MICHAELIS, Susan, 2018. Aircraft Clean Air Requirements Using Bleed Air Systems. In: *Engineering*, vol. 10, no. 4, pp. 142-172.
Available from: <https://doi.org/10.4236/eng.2018.104011> (Open Access)
- MTU AREO, 2020. *GE90-110B/-115B*.
Available from: <https://bit.ly/2Uqgynb>
Archived at: <https://perma.cc/Q6XZ-DZKY>
- MTU MAINTENANCE, 2020. *V2500 A1 & A4/D5 Familiarization*
Available from: <https://bit.ly/33F6uus>
Archived at: <https://perma.cc/4KG4-R27C>
- MURAWSKI, J. T. and SUPPLEE, D. S., 2008. An Attempt to Characterize the Frequency, Health Impact, and Operational Costs of Oil in the Cabin and Flight Deck Supply Air on U.S. Commercial Aircraft. In: *Journal of ASTM International*, Vol. 5, No. 5, pp. 1-15.
Available from: <https://doi.org/10.1520/JAI101640>
Archived at: <https://perma.cc/5U72-S3SF>
- OTIS, Charles E., 1997. *Aircraft Gas Turbine Powerplants*. Englewood: Jeppesen

PRATT & WHITNEY, 2014. *PW 4000-94 Inch Fan Engine*

Available from: <https://unitedtech.co/2J3FIIt>

Archived at: <https://perma.cc/6QJ6-BWUX>

SCHOLZ, Dieter, 2017. Aircraft Cabin Air and Engine Oil – An Engineering View. In: *International Aircraft Cabin Air Conference*, Imperial College, London, 20. September 2017.

Available from: <https://bit.ly/2vJXfgg> (Open Access)

SCHOLZ, Dieter, 2018. *Jet Engines – Bearings, Seals and Oil Consumption*. Hamburg, Germany.

Available from: <http://reports-at-aero.profscholz.de> (Open Access)

SMARTCOCKPIT, 2020. *Embraer 190 Powerplant*.

Available from: http://www.smartcockpit.com/docs/Embraer_190-Powerplant.pdf

Archived at: <https://perma.cc/UR79-REQ3>

TRAEGER, Irwin, 1995. *Aircraft Gas Turbine Engine Technology* 3rd ed., New York: MC Graw Hill Companies

SUMNER, Gregory, 1997. *The Pratt & Whitney 4060: Power to the Future*. Kalamazoo: Western Michigan University

Available from: <https://bit.ly/2y0vbpG> (Open Access)

Archived at: <https://perma.cc/QKB3-XCRR>

WILLENBORG, K. et al, 2006. Experimental Analysis of Air/Oil Separator Performance. In: *ASME Turbo Expo 2006: Power for Land, Sea, and Air. Volume 3: Heat Transfer, Parts A and B*. Barcelona, May 8-11

Available from: <https://doi.org/10.1115/GT2006-90708>